LC-DET-2005-004
May 31, 2005

Luminosity Measurement via Bhabha Scattering: Precision Requirements for the Luminosity Calorimeter

Achim Stahl
DESY[1]
Platanenallee 6
15738 Zeuthen
Germany

Achim.Stahl@desy.de

Abstract

At a future linear collider the luminosity will be measured from Bhabha scattering. The achievable precision will be limited by the reconstruction of the scattered particles in the luminosity calorimeter. In this note the required precision of reconstruction is estimated.

[1] Now at RWTH Aachen, Germany

1 Introduction

At a future linear collider the luminosity will be determined from the counting rate of Bhabha events and a theoretical calculation of the Bhabha cross section.

$$\mathcal{L}_{\text{int}} = \mathrm{N}_{\text{Bhabha}} \,/\, \sigma_{\text{Bhabha}} \tag{1}$$

$\mathcal{L}_{\text{int}}$ is the luminosity accumulated during the data taking period, $\mathrm{N}_{\text{Bhabha}}$ is the number of Bhabha events identified within a certain acceptance region, and σ_{Bhabha} the corresponding cross section calculated from theory. In a real experiment the identified sample of Bhabha events has to be corrected for background and efficiency and eqn. 1 needs to be modified to

$$\mathcal{L}_{\text{int}} = \frac{\mathrm{N}_{\text{Bhabha}} - \mathrm{N}_{\text{back}}}{\varepsilon} \,/\, \sigma_{\text{Bhabha}} \tag{2}$$

with the number of background events in the sample N_{back} and the selection efficiency ε. Most likely neither the background correction nor the efficiency correction will be a limiting factor in the luminosity measurement. I will ignore it here and work with eqn. 1.

Small angle Bhabha scattering will be used for the luminosity measurement with scattering angles in the range 30 to 75 mrad. The particles will be detected in LumCal (see fig. 1 and [2]). The characteristics of the Bhabha events is an electromagnetic cluster with full beam energy in the forward LumCal from the scattered electron and a corresponding one from the positron in the backward calorimeter[2]. The two clusters are back to back in azimuth and polar angle. In radiative events the energy of the clusters is reduced and additional clusters from photons might be detected. No tracking will be available in this region and therefore electrons cannot be identified from positrons. Photon showers might be identifiable from the absence of a signal in the first sensor plane, but we don't know yet, how well this will work.

The cross section for Bhabha scattering in this angular range is approximately 3 nbn at 500 GeV. With nominal luminosity ($3 \cdot 10^{34}/\mathrm{cm}^2\mathrm{s}$) approximately $9 \cdot 10^8$ events are collected in one year, enough to reach a statistical error of less than 10^{-4}. Figure 2 shows the development of the cross section with the center-of-mass energy [7].

It is hard to say which precision will finally be required, once the ILC is in full operation. Within the TESLA forward calorimeter collaboration, we have set ourselves a goal of an experimental error of $1 \cdot 10^{-4}$ [3]. The measurements at the ILC most sensitive to luminosity measurements are

- Measurement of the total hadronic cross section on the Z^0-resonance at GIGA-Z.
- The measurement of the cross section of 2-fermion production at high energy and with less precision the measurement of the $\mathrm{W}^+\,\mathrm{W}^-$cross section.
- The measurement of the production cross section of new resonances at high energy (W', Z', etc.), if such particles should be discovered.

There is a large theoretical effort ongoing to complete the full, massive, electroweak two-loop calculation of the Bhabha cross section [4]. If successful, it will result in a theoretical error of roughly the same size as the experimental error.

Luminosity measurement from Bhabha scattering has been used at $\mathrm{e}^+\,\mathrm{e}^-$ colliders before. The highest precision has been achieved by the two LEP experiments OPAL (exp. error $3.4 \cdot 10^{-4}$, theo. error $5.4 \cdot 10^{-4}$) [5] and ALEPH (exp. error $6.3 \cdot 10^{-4}$ in 1993, theo. error $6.1 \cdot 10^{-4}$) [6].

[2]The forward direction is defined as the direction of the electron beam.

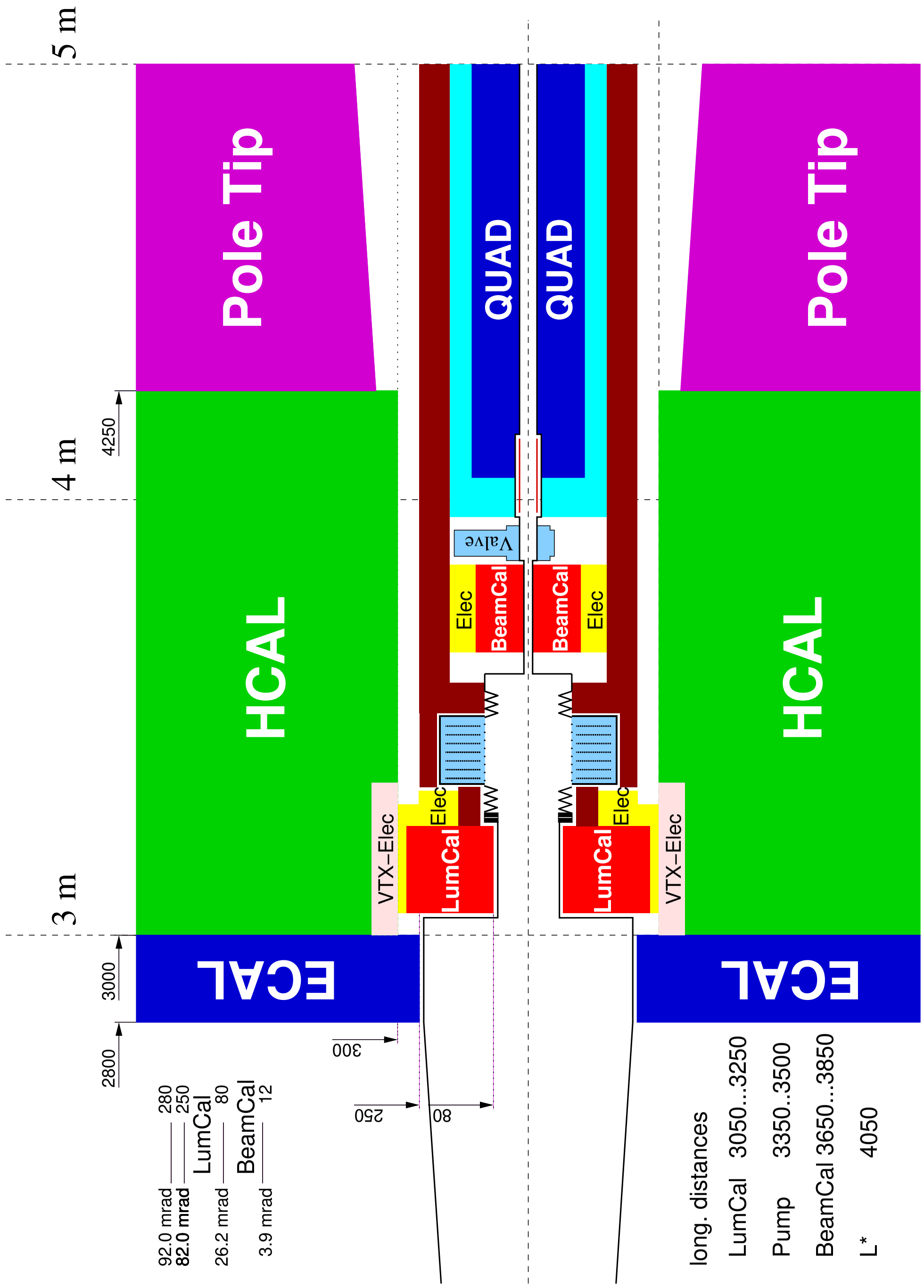

Figure 1: Preliminary redesign of the forward region for a focal length of the final focus between 4 and 5 meters.

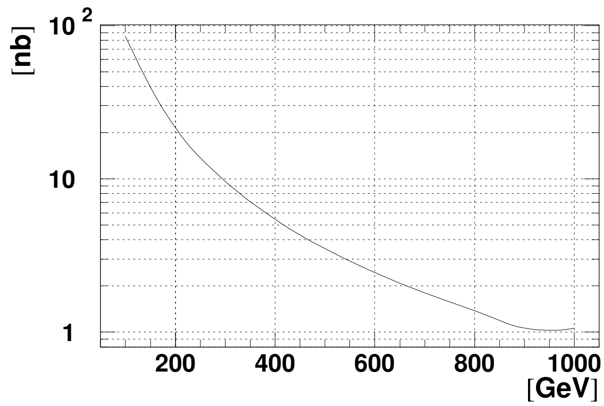

Figure 2: Visible cross section for the default cuts as a function of the center-of-mass energy (from BHLUMI).

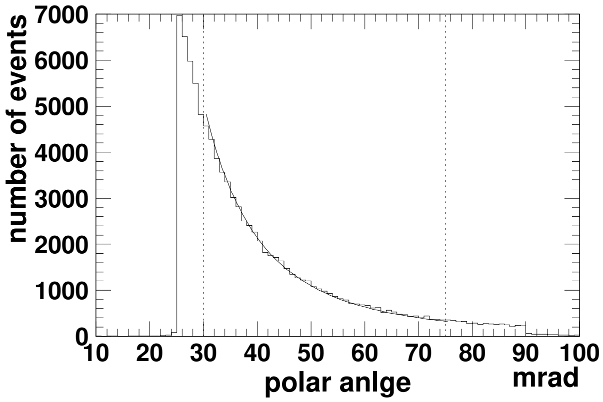

Figure 3: Polar angle distribution of positrons in small-angle Bhabha scattering calculated with BHLUMI. The dotted vertical lines indicate the accepted region. Events have been generated between 25 and 90 mrad. Entries outside this region are due to radiative corrections. The function represents the tree-level expectation $\sigma_{\mathrm{Bhabha}} \propto 1/\theta^3$. The statistics corresponds to approx. 20 minutes at nominal luminosity. Center-of-mass energy 500 GeV.

2 Simple, Analytic Estimates

The Bhabha cross section at small scattering angle is given to lowest order by[3]

$$\frac{\mathrm{d}\sigma_{\mathrm{Bhabha}}}{\mathrm{d}\Omega} = \frac{\alpha^2}{s} \frac{1}{\sin^4(\theta/2)} \approx \frac{16\,\alpha^2}{s} \frac{1}{\theta^4} \tag{3}$$

where α is the fine-structure constant and s the center-of-mass energy squared. For the luminosity analysis it is more appropriate to express the cross section in terms of the scattering angle θ:

$$\frac{\mathrm{d}\sigma_{\mathrm{Bhabha}}}{\mathrm{d}\theta} = \frac{2\pi\,\alpha^2}{s} \frac{\sin\theta}{\sin^4(\theta/2)} \approx \frac{32\,\pi\,\alpha^2}{s} \frac{1}{\theta^3}. \tag{4}$$

The angular distribution is illustrated in fig. 3. The cross section rises very rapidly with decreasing scattering angle θ, creating an experimental challenge: already small uncertainties in the knowledge of the accepted range of scattering angles will create a substantial

[3]The s-channel contributions of the photon and the Z^0 can be ignored for a rough estimate.

uncertainty in the measured luminosity. The scattering angle of the Bhabha events is reconstructed from the radial position of the detected clusters ($\mathrm{r}_{\mathrm{clus}}$) in the calorimeter and – with less sensitivity – from its distance from the IP (l_{LumCal}). Therefore the reconstruction of the radial position of a cluster in the LumCal and the radial dimensions of the calorimeter itself are most critical.

With $\theta_{\mathrm{clus}} \approx \mathrm{r}_{\mathrm{clus}}/l_{\mathrm{LumCal}}$ one gets

$$\frac{\Delta\mathcal{L}}{\mathcal{L}} = 2\,\frac{\Delta \mathrm{r}_{\mathrm{clus}}}{\mathrm{r}_{\mathrm{clus}}} \approx 2\,\frac{\Delta \mathrm{r}_{\mathrm{clus}}}{\theta_{\mathrm{min}}\, l_{\mathrm{LumCal}}} \tag{5}$$

where $\Delta\mathcal{L}$ indicates the error on the luminosity and $\Delta\mathrm{r}_{\mathrm{clus}}$ a systematic error on the reconstruction of the radial cluster position as for example a falsely measured radius of the calorimeter.

Similarly one gets for an error on the longitudinal position of the calorimeters

$$\frac{\Delta\mathcal{L}}{\mathcal{L}} = 2\,\frac{\Delta l_{\mathrm{LumCal}}}{l_{\mathrm{LumCal}}} \tag{6}$$

3 Method

Bhabha events are simulated with BHLUMI (version 4.04)[4] in the phase space region of the TESLA luminosity calorimeter [7]. The simulation is based on a redesign of the forward region for an l^* that allows to place the luminosity calorimeter behind the ECal endcap[5]. The luminosity calorimeter is called LumCal to distinguish it from the LAT and LCal of the TDR design. The design is sketched in fig. 1 (see [2] for more details).

A simple selection is applied to the simulated events (see below). In a first step the position of the electron and positron on the front face of LumCal is calculated. The scattering angles are determined from these positions. The energy of the particles is taken from the tree. In subsequent steps the position and energy are subjected to systematic misreconstructions and the selection is reapplied. The change in the number of accepted events with respect to step 1 gives the systematic error on the luminosity introduced by the respective misreconstruction. The size of the effects are varied in order to determine the level which is acceptable with a goal of 10^{-4} precision on the luminosity measurement. The same event sample is used for all steps so that statistical fluctuations largely cancel.

BHLUMI version 4.04 was used with the following parameters:

Type of generator	BHLUM4
Photon Removal	on
Event weights	off
Random generator	RANMAR
Z^0-contribution	on
QED matrix elements	from BHLUM4
Vacuum polarization	from ref. 1
center-of-mass energy	500 GeV
min. scattering angle	25 mrad
max. scattering angle	90 mrad
photon infrared cut-off	10^{-4}

The following cuts are applied to identify Bhabha events

- energy: $E\,(e^+) > 0.8\,E_{\mathrm{beam}}$
  $E\,(e^-) > 0.8\,E_{\mathrm{beam}}$
- scattering angle of positron or electron: $30\,\mathrm{mrad} < \theta < 75\,\mathrm{mrad}$

The cut on the scattering angle is applied to either electron or positron, but never both. For events with an even event number it is applied to the positron, for odd event numbers to

[4] S. Jadach and S. Waş, http://jadach.home.cern.ch/jadach/Welcome.html
[5] l^* is the focal length of the final focus system.

the electron, creating a quasi random (uncorrelated with event characteristics) alternation between the two. This largely reduces the sensitivity of the luminosity measurement to the longitudinal position of the interaction point.

Please notice, that even if the acceptance cut is applied only on one side, the energy cut still implies a weak cut on the recoil side. In order to pass the energy cut the recoiling particle has to be detected in the LumCal (26.2 to 82.0 mrad).

In the real situation it will not always be possible to uniquely identify the electron and the positron. Photons will interact nearby and their clusters might merge. In the real situation the most energetic cluster will be used as electron and positron. An investigation of the impact of this effect requires a full detector simulation. This has not been done here. I don't expect this to make a substantial difference.

It is important to keep the area in front of the calorimeters free of material. Any material, even small things like cables, will introduce scattering and energy loss of the electrons and positrons and will reduce the angular and energy resolution of the detectors. As these materials are hard to simulate exactly they can easily become a limiting factor of the precision. The new design [2] fullfils this requirement. There is no material in front of LumCal except for the exit window from the beam pipe.

4 Findings

4.1 Inner diameter of LumCal

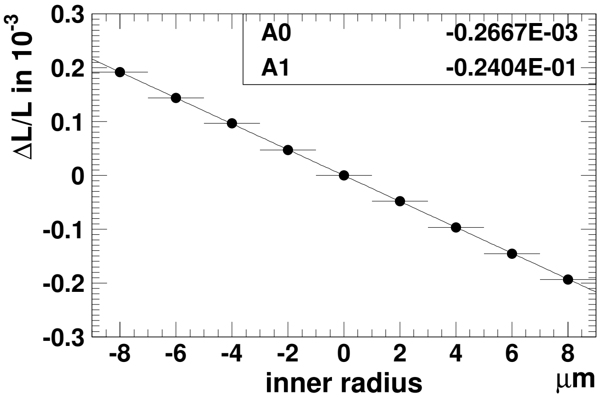

Figure 4: Systematic impact on the luminosity measurement due to a mismeasurement of the radius of the calorimeter. The x-axis gives the deviation of the true radius of the detector from the radius assumed in the analysis. Center-of-mass energy 500 GeV.

The most critical parameter is the diameter of the calorimeter (see fig. 4), i.e. the distance across the beam pipe from on side of the calorimeter to the other. To simulate this effect the reconstructed radius of each shower has been increased by the amount indicated on the plot identically for the forward and backward calorimeter. The systematic error increases linearly with the error on r_{clus} with a slope of $0.24 \cdot 10^{-4}/\mu$m. If only one calorimeter is affected the impact is reduce by a factor of 2. From the slope one calculates that the inner radius has to be controlled to better than $4\,\mu m$. The simplified calculation from eqn. 5 gives $4.6\,\mu m$.

This applies to the sum of the uncertainties of the mechanical dimension of calorimeter (or more precisely the mechanical precision of the sensors defining the acceptance cut) and any bias in the reconstruction of the shower position. Such biases could arise from reconstruction algorithm (typically they bias towards the center of a pad), the shape of the pads, the non-perpendicular impact of the particles, transverse shower leakage at the inner edge of the calorimeter, variations in gain between pads, and others.

The effect has been calculated for a center-of-mass energy of 500 GeV. To first order it is independent of the center-of-mass energy.

For the luminosity analysis at LEP the mechanical precision of the detector radius has been the limiting factor of the experimental precision [6, 5]. OPAL achieved a precision of 4.4 μm on the calorimeter contributing $1.4 \cdot 10^{-4}$ to a total experimental error of $3.4 \cdot 10^{-4}$ (see table 6 in [5]).

4.2 Radial beam position

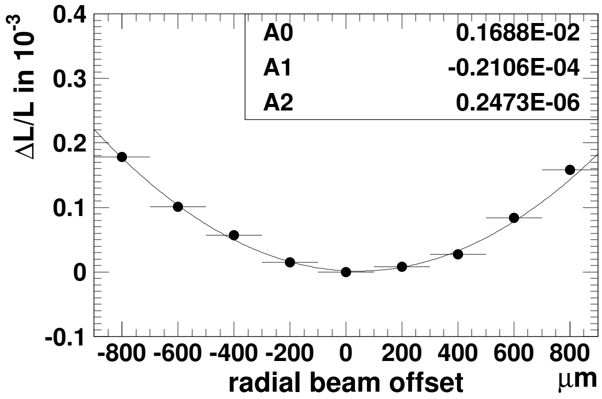

Figure 5: Systematic impact on the luminosity measurement due to a radial offset of the position of the beam. Center-of-mass energy 500 GeV.

Fig. 5 shows a radial mispositioning of the detector with respect to the beam. The detector axis is offset from the beam axis by the amount indicated. Comparison with fig. 4 shows that this parameter is less critical. The dependence is quadratic and severe effects only appear on the scale of hundreds of microns. This can be understood directly. If one would restrict the measurement to a fixed azimuthal angle ϕ the effect of a change in radius of the calorimeter and a radial mispositioning of the detector would be the same. But, we do integrate over the full azimuthal angle. The effect of section 4.1 adds up for all azimuthal angles, while the effect of this section cancels between opposite sides. Let's say the beam is offset in the +x direction, then one gains events around $\phi = 0°$, but one looses events around $\phi = 180°$. The effect cancels to first order and therefore depends quadraticly on the offset.

The fit shows that it is sufficient to know the beam position to a few hundred μm. It should not be a problem to determine the beam position to that accuracy from the BPMs (beam position monitors) of the fast feedback system. Furthermore it can be measured from the Bhabhas themselves. An offset of the beam creates an azimuthal asymmetry in the Bhabha rate from which the offset can be extracted. Alternatively one can draw (event-by-event) a straight line connecting the electron position with the positron position. By overlaying the lines from all events one reconstructs the luminous region and with it the beam offset.

4.3 Longitudinal distance of forward and backward calorimeter

The second most critical parameter besides the inner radius is the distance between the forward and backward calorimeter along the z-axis. If the two detectors are closer to each other than expected, the same shower position reflects a slightly larger scattering angle and therefore a slightly smaller Bhabha cross section.

Fig. 6 shows the change in the extracted luminosity as a function of the error on the half-distance between the two calorimeters. The plot shows a linear dependence with a

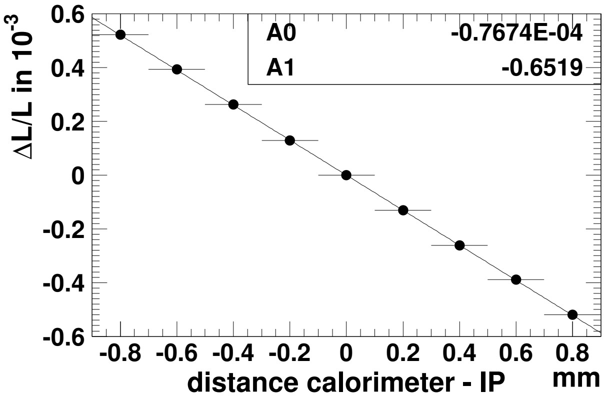

Figure 6: Systematic impact on the luminosity measurement due to an error in the half-distance between the two calorimeter. The nominal half-distance (IP to calorimeter) is 3050 mm. The two calorimeter are offset from each other by twice the amount indicated on the x-axis. Center-of-mass energy 500 GeV.

slope of $0.65 \cdot 10^{-4}/100\,\mu$m consistent with the estimate from eqn. 6. The alignment must be controlled at least to 100 μm over a distance of 3 m.

4.4 Longitudinal offset of the interaction point

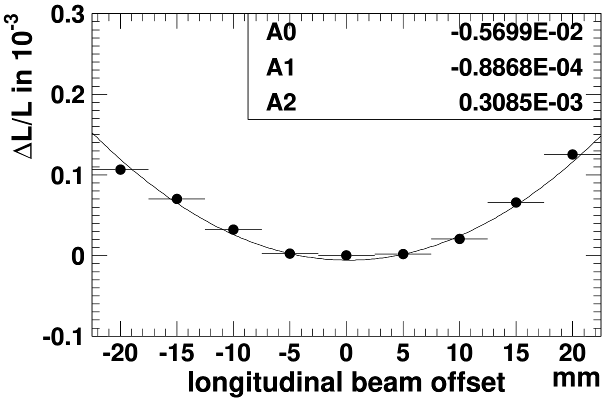

Figure 7: Systematic impact on the luminosity measurement due to a longitudinal offset of the interaction point from the center of the detector.

The figure shows the effect on the luminosity measurement of an offset of the interaction point from the center of the detector along the beam direction. The dependence is quadratic with a coefficient of $0.3 \cdot 10^{-4}/\mathrm{cm}^2$. It is sufficient to determine the longitudinal position of the interaction point to 1 cm. That should be easy to achieve.

Such a low sensitivity to the longitudinal position of the IP is a consequence by the acceptance cut applied to either electron or positron, alternating from event to event. If one would apply the cut to the electron only for every event, one would get the same sensitivity as for the previous section (longitudinal distance of calorimeters). Assume the IP is offset in the +z-direction. Than in events where the cut is applied to the electron in the forward calorimeter, the calorimeter is too close and the reconstructed polar angle is too small. Events just inside the accepted range will get falsely rejected. But for events where the cut is applied on the backward calorimeter the effect is reversed. The calorimeter is too far away, the reconstructed angle too large and too many events are accepted. The two effects cancel to first order. Only the much reduced second order sensitivity remains.

Applying the acceptance cut for each event symmetrically on electron and positron is also not a good idea. One would get the same linear dependence as in the previous section, but with a different sign for positive and negative offsets.

4.5 Tilt of the calorimeters

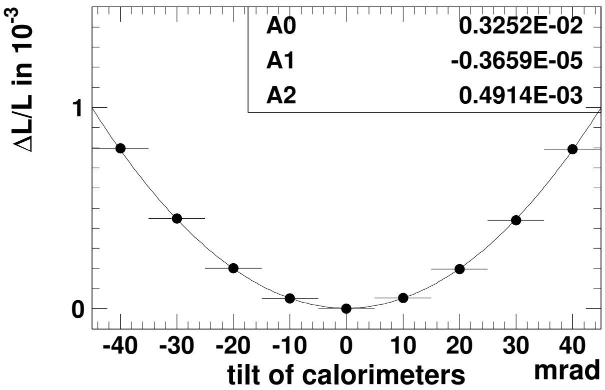

Figure 8: Systematic impact on the luminosity measurement from a tilt of the calorimeters with respect to the beam axis. Here both detectors have been tilted around the y-axis in the same direction.

Figure 8 shows the error in the luminosity measurement introduced, if the calorimeter are placed not exactly perpendicular to the beam axis. In the figure the two calorimeters are rotated around the y-axis in the same direction. With a tilted calorimeter each particle will impact at a slightly larger radius and a larger polar angle is reconstructed. The number of accepted events and therefore the measured luminosity increases. The quadratic behavior comes from the translation of rotation angle into radial position:

$$\mathrm{r_{clus}} \rightarrow \frac{\mathrm{r_{clus}}}{\cos\phi_{\mathrm{tilt}}} \approx \mathrm{r_{clus}} \cdot (1 + \frac{1}{2}\phi_{\mathrm{tilt}}^2) \tag{7}$$

The quadratic coefficient from the simulation is $0.5 \cdot 10^{-4}/(10\,\mathrm{mrad})^2$. The effect of such a rotation is independent of the axis of rotation. A rotation of the two calorimeters in the same direction gives the same sensitivity as a rotation in opposite direction as does a rotation of one calorimeter around the x-axis and the other around the y-axis.

The tolerance on the alignment of each calorimeter with respect to the beam direction must be better than ± 10 mrad. This should not be too difficult to achieve. At 10 mrad the outer edge of the calorimeter has already moved by 2.5 mm which should be readily detected by the longitudinal position monitoring system (assuming we have more than one measurement at different azimuthal angles).

4.6 Twist between the two calorimeters

Another systematic effect might arise from a rotation of the calorimeters around the beam direction. This would effect the reconstruction of the azimuthal angles of electron and positron. In the analysis presented here this would have no effect. The azimuthal angles are not used in the selection. The difference in the azimuth between electron and positron ($\Delta\phi$) should be equal to π for non-radiative events[6]. Figure 9 shows the deviation from π due to radiative corrections. In a real situation one might want to place a cut on $\Delta\phi$ for two reasons. It could be used to reduce the background in the Bhabha sample and to remove

[6]Except for a small shift due to the magnetic field

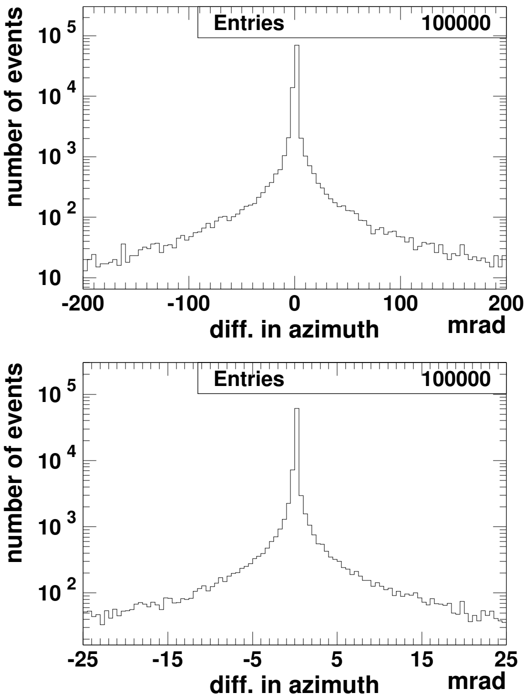

Figure 9: The difference $\Delta\phi$ in azimuthal angle between the forward and the backward shower. A value of π has been subtracted to center the distribution around 0. The two plots show different regions in $\Delta\phi$.

radiative tails. These tails are harder to calculate and the theoretical error can usually be reduced by cutting the radiative tails.

It is hard to estimate what a proper value for a cut on $\Delta\phi$ will be. As a very rough estimate, I give the numbers for a cut of 20 mrad, which is probably a very tight cut. Such a cut will remove almost 10 % of the events from the sample. In order to reduce the corresponding systematic error below 10^{-4} the measurement of the azimuthal angles and with it the orientation of the calorimeters needs to be measured to a precision of 0.1 mrad. This might sound challenging, but one can use the peak at $\Delta\phi = \pi$ to calibrate the measurement. With a less stringent cut the requirements are quickly relaxed. Overall I don't expect a substantial problem here.

4.7 Beam tilt

If the two beams reach the IP not exactly along the nominal beam axis the effect shown in fig. 10 will appear. Both beams are assumed to be rotated so that they still collide head-on.

It is sufficient to control this rotation to 0.1 mrad. At such an angle the beams are already offset in the BPMs by about 400 μm which should be easily detectable.

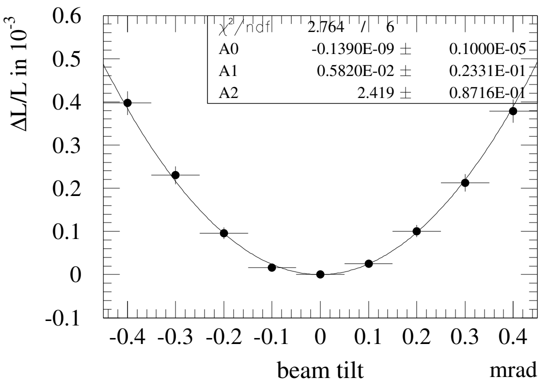

Figure 10: Systematic impact on the luminosity measurement due to a non-vanishing angle between the beam axis and the detector axis.

4.8 Beam size at the IP

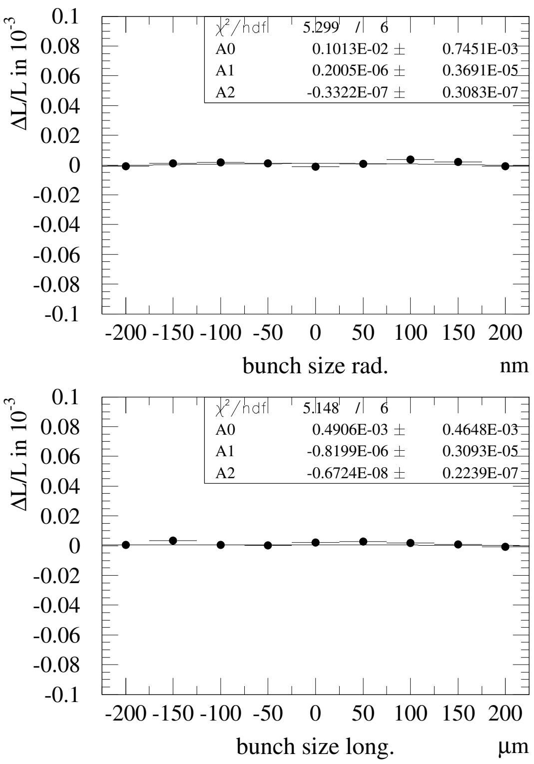

Figure 11: Systematic impact on the luminosity measurement due to a deviation of the horizontal spot size at the IP from its nominal value of 553 nm (left) and of the longitudinal spot size from its nominal value of 300 μm (right).

The beams of TESLA have a transverse size of 5 nm by 553 nm and a longitudinal size of 300 μm at the IP. Figures 11 shows the influence of the spacial extension of the luminous region. No relevant variation is visible (this was different at LEP). Therefore all other plots are generated with point-like interaction region.

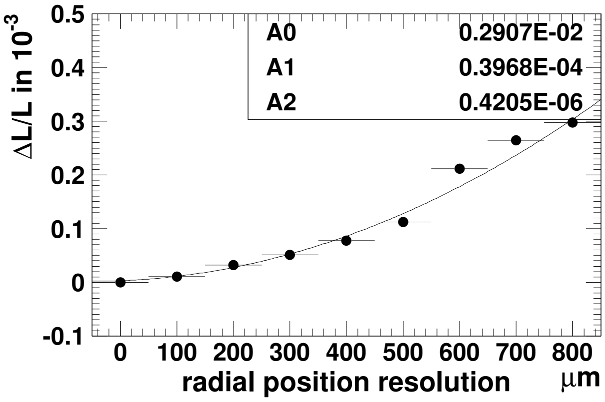

Figure 12: Systematic impact on the luminosity measurement due to the resolution in radial shower position of the calorimeters.

4.9 Position resolution

Figure 12 shows the impact of the finite position resolution of the detector. Particles just outside the fiducial volume can be mismeausred to be inside and vice versa. Due to the steeply rising cross section at the inner acceptance border, more events will leak in than sneak out. An artificial increase in the number of detected events is expected. In fact for a sample of 10^7 events reconstructed with a radial resolution of $100\,\mu$m 8283 events were incorrectly reconstructed inside the fiducial volume and 8145 were incorrectly lost from the fiducial volume. At this resolution, the overall effect is negligible. The dependence of the visible cross section on the position resolution is quadratic with a second order coefficient of $4 \cdot 10^{-6}/(100\,\mu\mathrm{m})^2$. At $500\,\mu$m resolution the visible cross section has changed by 10^{-4} compared to an ideal detector.

This does not imply that the position resolution has to be better than 500μm, because the effect can be corrected. How well it has to be corrected depends on the position resolution itself. If it is good, the correction is not critical. It becomes critical if the resolution is worth than $500\,\mu$m. Quantitatively it is given by the first derivative of the quadratic fit function. An error in the knowledge of the position resolution will lead to an error on the luminosity measurement of

$$\frac{\Delta\mathcal{L}}{\mathcal{L}} = 8 \cdot 10^{-6} \cdot \frac{\sigma_\mathrm{r}}{100\,\mu\mathrm{m}} \cdot \frac{\Delta\sigma_\mathrm{r}}{100\,\mu\mathrm{m}}. \tag{8}$$

Here σ_r is the position resolution and $\Delta\sigma_\mathrm{r}$ the uncertainty in the knowledge of the position resolution. For example with a position resolution of $500\,\mu$m, known to 20 % we would get an uncertainty in the luminosity of $0.4 \cdot 10^{-4}$. This should be a manageable task.

4.10 Energy resolution and calibration

Figure 13 shows the spectrum of the electrons scattered into the fiducial volume. On the right side the scatter plot of electron versus positron energy can be seen. The long tails from radiation are clearly visible. In most cases of radiation either the electron or the positron is affected, but not both, indicating that final state radiation dominates. This is mostly an experimental effect. Events with initial state radiation are accollinear. With the small detectors it is unlikely that electron and positron are both detected in LumCal. Beamstrahlung will create additional low-energy tails which are not taken into account here.

Any mistake in the measurement of the energy of the electron or positron changes the efficiency of the first selection cut ($E > 0.8\,E_\mathrm{beam}$). The situation is similar to the potential cut on $\Delta\phi$ (see sec. 4.6): A cut on the electron and positron energy will be necessary to separate the Bhabha signal from the background. The background is currently not known and therefore the cut value is just a guess. It is set at 80 % of the beam energy (box in fig. 13).

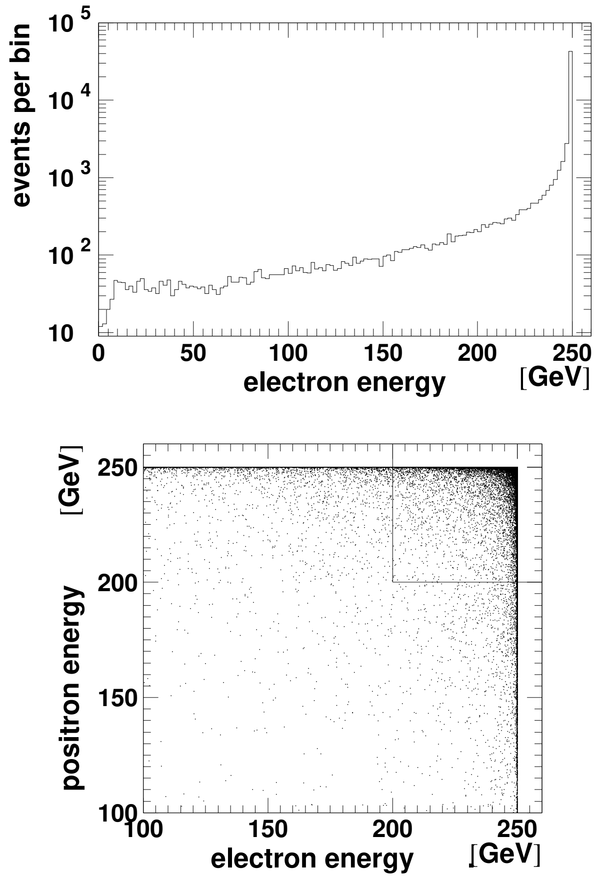

Figure 13: Energy spectrum of electrons scattered into the fiducial volume (acceptance cut applied on the electrons).

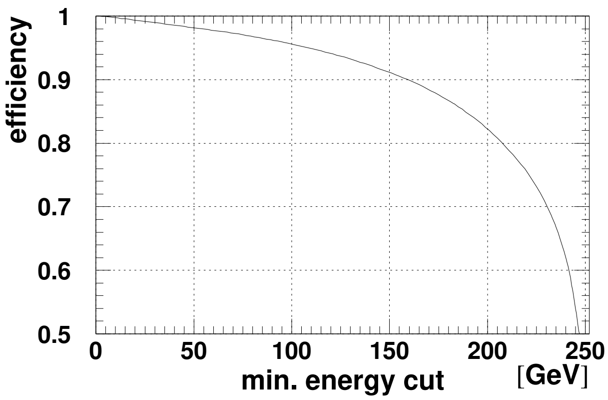

Figure 14: Efficiency of the selection cut on the electron and positron energy versus the cut value. The cut is always applied on the electron and the positron energy. The default cut is at 200 GeV.

Figure 14 indicates how the efficiency changes with the value of the energy cut. At the nominal value of 80 %, corresponding to 200 GeV, the efficiency is 82.52 %. The slope of the efficiency at this point is $2.7 \cdot 10^{-3}$/GeV. If one manages to understand the calibration of the detector to 10^{-4}, this still gives a contribution to the systematic error of $0.7 \cdot 10^{-4}$. This

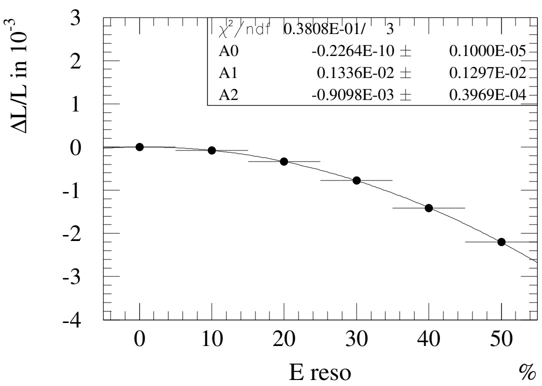

Figure 15: Systematic impact on the luminosity measurement from the calibration of the calorimeter.

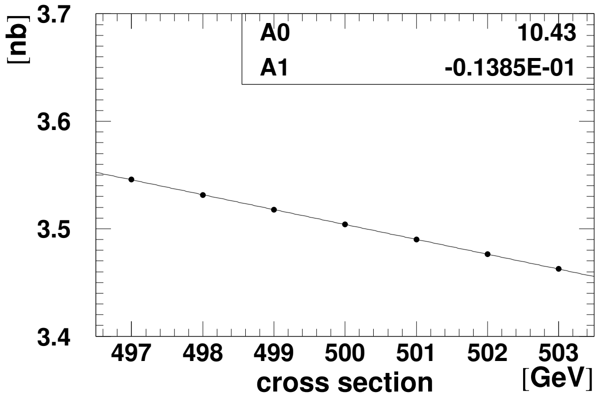

Figure 16: Visible cross section for the luminosity analysis in the vicinity of the nominal center-of-mass energy.

is a challenge, even with the self calibration through the Bhabha peak. If the background is less severe, the energy cut can be lowered and the sensitivity is reduced. Introducing an accollinearity cut would also reduce this sensitivity.

Also a finite energy resolution influences the luminosity measurement. A dependence of the resolution of the form $\frac{\sigma_E}{E} = \frac{a}{\sqrt{E}}$ is assumed. Figure 15 shows how the measured luminosity depends on the coefficient a (given in %). Again the true sensitivity changes with the value of the energy cut. Tighter cuts create a higher sensitivity. The dependence is quadratic with a coefficient of $-9 \cdot 10^{-7}\ a^2$ (a in %). With a resolution of $20\ \%/\sqrt{E}$ the correction to the luminosity would be $3.6 \cdot 10^{-4}$. How well this correction needs to be understood is determined by the derivative of the quadratic dependence. One gets:

$$\frac{\Delta\mathcal{L}}{\mathcal{L}} \approx -2 \cdot 10^{-6} \cdot a \cdot \Delta a \tag{9}$$

where Δa is the uncertainty in the coefficient a (in %). The energy resolution must be understood to at least 2 % for a resolution of $20\ \%/\sqrt{E}$. This should be feasible. If the energy resolution is better than $20\%/\sqrt{E}$ (this is quite a pessimistic value), the requirement is relaxed.

4.11 Center-of-Mass Energy

The cross section for Bhabha scattering changes with the center-of-mass energy roughly as 1/s. For an overview see fig. 2. Figure 16 shows the cross section for the luminosity after all cuts in the vicinity of our default center-of-mass energy of 500 GeV. In this small range the cross section can be approximated by a straight line with a slope of -0.014 nbn/GeV. To determine the luminosity the center-of-mass energy must be precisely known. To reduce the corresponding uncertainty below 10^{-4} the center-of-mass energy must be known to 25 MeV or $5 \cdot 10^{-5}$. Most likely it will not be possible to determine the center-of-mass energy with such a precision. But now we have to go one step further. In the end we want to use the luminosity measurement to determine unknown cross sections of other interesting processes. These cross sections also have an s-dependence. In many cases it is similar to that of the Bhabha cross section and the error introduced by the uncertainty in the center-of-mass energy will cancel[7]. This is the case for example for any s-channel process far away from resonances. In other situations the impact will be enhanced, for example on the slope of a threshold. Whether the knowledge of the center-of-mass energy presents a problem depends on the individual analysis somebody is trying to do.

4.12 Comparison to TDR design

The design of the LumCal and the forward region used here is the new design from [2]. It differs substantially from the design presented in the Technical Design Report [1]. Besides the shape of the luminosity calorimeter the main difference for the luminosity measurement is the change of the distance of the calorimeters from the IP. For the new design this distance is 3.05 m, while it was 2.0 m in average for the TDR design.

In tab. 1 the requirements on the knowledge of the various parameters discussed in the previous sections are compared for the two designs. For each parameter two numbers are given. In the right column the requirement to reduce the impact of this single effect to $\Delta\mathcal{L}/\mathcal{L} = 10^{-4}$ is given. This number is the overall goal in luminosity precision. In the left column the requirement to reduce the impact to $\Delta\mathcal{L}/\mathcal{L} = 0.2 \cdot 10^{-4}$ is also given. At this point the effect become essentially negligible. The number quoted for the position resolution corresponds to the required knowledge of a 500 μm resolution.

One can clearly see that the larger distance from the IP in the new design relaxes the requirements somewhat. For the two most critical parameters the inner radius of the detectors (sec. 4.1) and the distance between the two calorimeters (sec. 4.3) the tolerances are larger by about 50 %.

[7] One still has to make sure that the same s' range is used for unknown process and the Bhabha scattering or one has to correct for the difference.

	TDR		new	
$\Delta\mathcal{L}/\mathcal{L}$	$0.2 \cdot 10^{-4}$	$1.0 \cdot 10^{-4}$	$0.2 \cdot 10^{-4}$	$1.0 \cdot 10^{-4}$
inner radius	0.5 μm	2.7 μm	0.8 μm	4.2 μm
radial offset	180 μm	400 μm	290 μm	640 μm
distance of calos	40 μm	200 μm	76 μm	300 μm
long. offset	5 mm	11 mm	8 mm	18 mm
tilt of calo	6 mrad	14 mrad	6 mrad	14 mrad
beam tilt	0.28 mrad	0.63 mrad	0.28 mrad	0.63 mrad
beam size	negligible			
position reso.	3 %	15 %	10 %	48 %
energy reso.	identical			
beam energy	identical			

Table 1: Comparison of the precision requirements for the luminosity measurement between the TDR design [1] and the new design [2].

5 Conclusion

At the future linear collider luminosity will be precisely measured from small angle Bhabha scattering. It has been studied here, what the limiting factors in the experimental precision will be. The new design of the forward region of the TESLA detector has been chosen as an example. Similar results are expected for any detector design with a similar geometrical acceptance of the luminosity calorimeter.

The statistical precision of the Bhabha counting will be sufficient to reach the goal of an experimental error of not more than $\Delta\mathcal{L}/\mathcal{L} = 10^{-4}$. It turns out the most critical systematic effect is the knowledge of the radial size of the calorimeter. The diameter of the inner border of acceptance must be know at least to 8 μm or the radius to 4 μm. Critical is also the distance between the two calorimeters along the beam axis (required precision 200 μm). For some cross section measurements the knowledge of the center-of-mass energy might also be a limiting factor.

References

[1] TESLA Technical Design Report, DESY 2001-011, ECFA 2001-209, March 2001. For the forward regions see Vol. IV, sec. 3.5 and 7.1.

[2] K. Büßer, A. Stahl, *Detector Concept for the Forward Regions*, LC-DET-2004-034.

[3] DESY proposal, PRC November 2002, *R&D for the TESLA Detector: Instrumentation of the very forward region*, (http://www-zeuthen.desy.de/~astahl/Collaboration.html).

[4] See for example: http://www-zeuthen.desy.de/theory/research/bhabha/

[5] OPAL, G. Abbiendi et al., Eur. Phys. J C14 (2000) 373.

[6] ALEPH, R. Barate et al., Eur. Phys. J C14 (2000) 1.

[7] S. Jadach, E. Richter-Was, B. F. L. Ward and Z. Was, Comp. Phys. Comm. **102** (1997) 229.